Fermi arc in the superconducting state of impurity-doped Bi2Sr2CaCu208

doi: 10.1103/PhysRevB.78.100502

PHYSICAL REVIEW B **78**, 100502(R) (2008)

Fermi arc in the superconducting state of impurity-doped $Bi_2Sr_2CaCu_2O_8$

T. Sato,[1] K. Terashima,[1] K. Nakayama,[1] S. Souma,[2,3] T. Takahashi,[1,2,3] T. Yamamoto,[4] and K. Kadowaki[4]
[1]*Department of Physics, Tohoku University, Sendai 980-8578, Japan*
[2]*CREST, Japan Science and Technology Agency (JST), Kawaguchi 332-0012, Japan*
[3]*WPI Research Center, Advanced Institute for Materials Research, Tohoku University, Sendai 980-8577, Japan*
[4]*Institute of Materials Science, University of Tsukuba, Tsukuba 305-8573, Japan*
(Received 4 July 2008; published 4 September 2008)

We have performed ultrahigh energy- and momentum-resolved angle-resolved photoemission spectroscopy of impurity-doped $Bi_2Sr_2CaCu_2O_8$. We found that the point node of the superconducting gap near the $(\pi/2,\pi/2)$ point in a pristine sample gradually evolves into a small gapless Fermi arc upon Zn or Ni doping. The shape of impurity-induced density of states inside the superconducting gap shows a marked difference between Zn and Ni doping, demonstrating that the low-energy excitation properties are strongly sensitive to the character of impurities.

DOI: 10.1103/PhysRevB.78.100502 PACS number(s): 74.72.Hs, 71.18.+y, 74.25.Jb, 79.60.Bm

The ground-state properties of high-temperature superconductors such as the superfluid density and the pairing symmetry have been intensively studied since they are closely related to the pairing mechanism. One of the most effective approaches to elucidate the pairing state is to dope impurities in the crystal as applied in conventional superconductors.[1] It is well known that the nonmagnetic- or magnetic-impurity substitution in high-temperature superconductors causes a drastic decrease in the superconducting (SC) transition temperature (T_c) and at the same time substantially influences the macroscopic transport and thermodynamic properties in both the SC and normal states. Recent scanning tunneling microscopy/scanning tunneling spectroscopy (STM/STS) studies have revealed that impurities produce the bound state within the SC gap due to the strong scattering of holes around the impurity site.[2,3] The anomalous spatial distribution of tunneling density of states (DOS) around the impurity and the marked difference between Zn and Ni doping have suggested an unconventional mechanism beyond the simple potential scattering, stimulating active discussions on the microscopic origin of the impurity bound state and its relation to the pairing symmetry.[4] In contrast, the impurity effect in the momentum (k) space has not been well unraveled,[5–8] although the k-space information is also essential to reveal the nature of pairing state by complementing the real-space information by STM/STS. To observe a presumably small impurity effect in the k space, the ultrahigh momentum resolution in addition to the high energy resolution is necessary in angle-resolved photoemission spectroscopy (ARPES) like the ultrahigh spatial resolution in STM.

In this Rapid Communication, we report ultrahigh momentum- and energy-resolved ARPES on Zn- or Ni-substituted $Bi_2Sr_2CaCu_2O_8$ (Bi2212) with a newly developed xenon (Xe) plasma light source.[9] The ultrahigh momentum resolution (<0.004 Å^{-1}, about 1/400 of the Brillouin-zone size) is achieved by combination of the high angular resolution of the spectrometer and the relatively low photon energy of the Xe resonance line. In addition, ARPES with the Xe light source has a great advantage of the higher bulk sensitivity. We have precisely measured single-particle excitation spectra in the vicinity of the Fermi level (E_F) and found several distinct impurity effects on the SC gap in the k space, such as the recovery of the Fermi arc around $(\pi/2,\pi/2)$, the emergence of bound states inside the SC gap, and the marked difference between Zn and Ni doping.

High-quality single crystals of nearly-optimally doped pristine and impurity-substituted Bi2212 were grown by the traveling-solvent floating zone method. The content of Zn or Ni impurity was estimated to be 0.5–1.0% by the electron probe microanalysis together with the decrease in T_c of substituted samples. The T_c value is 90 K for a pristine sample and 80–85 K for substituted samples. Ultrahigh-resolution ARPES measurements were performed using a VG-SCIENTA SES2002 photoemission spectrometer using a newly developed Xe plasma light source.[9] Since electrons near E_F excited by the Xe I resonance line ($h\nu$=9.570 eV) have a relatively long escape depth (20–40 Å), the photoemission spectrum largely reflects the bulk electronic structure. We used nonmonochromatized Xe lines. These lines contain mainly 8.437-, 9.570-, 9.917-, and 9.961-eV photons with the relative intensity of 100, 18, 8.6, and 1.6%, respectively.[9] The reason why we used 9.570-eV photons is to cover a wider momentum area with a reasonable count rate. We found that the ARPES spectrum near E_F measured with the 9.570-eV photons contains featureless background of less-than-10% intensity with respect to the main peak. The background originates in the higher-energy photons (mainly $h\nu$=9.917 and 9.961 eV), and has been subtracted by assuming a constant offset. The energy and angular (momentum) resolutions were set at 4 meV and 0.2° (0.004 Å^{-1}), respectively. We cleaved samples under ultrahigh vacuum of 2×10^{-11} Torr to obtain a clean and fresh sample surface for ARPES measurements. The Fermi level (E_F) of samples was referenced to that of a gold film evaporated onto the sample substrate. We have confirmed the reproducibility of experimental data by measuring several samples.

Figure 1(a) shows the plot of ARPES intensity around E_F for pristine Bi2212 as a function of two-dimensional wave vector, measured at 10 K with one of Xe I resonance lines (9.570 eV). We find a large Fermi surface centered at the (π,π) point in the Brillouin zone in good agreement with previous reports with higher-energy photons.[10] Figure 1(b) displays the momentum distribution curve (MDC) at 20-meV binding energy along a cut slightly away from the node [cut

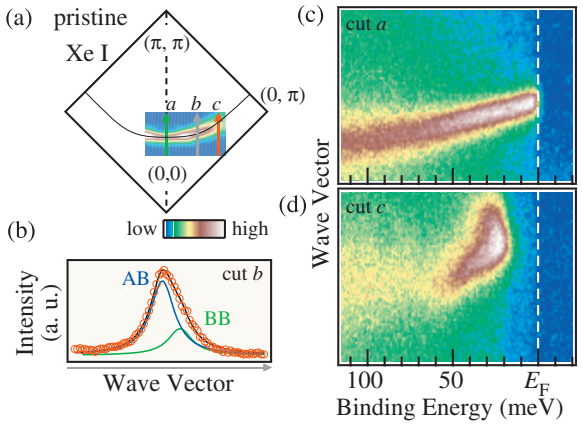

FIG. 1. (Color) (a) ARPES intensity at E_F plotted as a function of 2D wave vector for pristine Bi2212, measured at 10 K with the Xe I resonance line ($h\nu$=9.570 eV). The spectral intensity was integrated within ±40 meV with respect to E_F, and normalized by the photon flux. (b) MDC at 20-meV binding energy measured for cut *b* in (a). (c) and (d) ARPES-intensity plot near E_F as a function of wave vector and binding energy measured along the nodal (cut *a*) and the off-nodal cut (cut *c*), respectively.

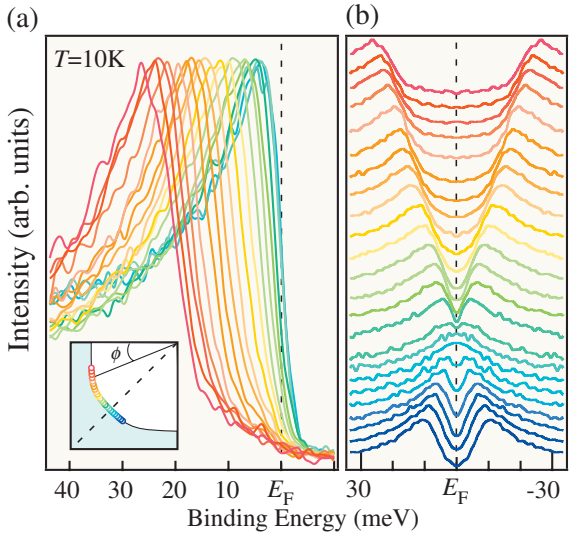

FIG. 2. (Color) (a) ARPES spectra for pristine Bi2212 measured at 10 K at several k_F points of the antibonding band. Location of k_F points is indicated by differently colored circles in the Brillouin zone (inset). (b) Symmetrized ARPES spectra in (a).

b in Fig. 1(a)]. The MDC looks asymmetric with respect to the peak top, and is well fitted with two Lorentzians which correspond to a predominant antibonding band (AB) and a weaker bonding counterpart (BB)[11,12] produced by the interaction between two CuO_2 planes in a unit cell. Figures 1(c) and 1(d) show ARPES-intensity plots at 10 K as a function of binding energy and wave vector for the nodal cut (cut *a*) and the off-nodal cut (cut *c*) located midway between the node and the $(\pi,0)$ point. Along cut *a*, a highly dispersive band with a small kink at about 70 meV crosses E_F, while along cut *c*, the band does not cross E_F and disperses back toward higher binding energy because of the SC-gap opening. These features are essentially similar to the previous ARPES reports with higher-energy photons,[13,14] demonstrating that the so-far revealed $d_{x^2-y^2}$-wave SC gap and the Bogoliubov-type character of quasiparticle (QP) are intrinsic features of bulk properties.

Figure 2(a) displays the 10-K ARPES spectra measured at various Fermi vector (k_F) points of the antibonding band indicated by circles in the Brillouin zone (inset). At the nodal k_F point (light blue spectrum), the leading-edge midpoint is situated slightly above E_F, showing the closure of a SC gap at the nodal k_F point. When we move slightly away from the node, the leading edge immediately starts to shift toward higher binding energy, suggesting the existence of a point node. It is remarked that the position of the QP peak and leading edge is considerably sensitive to even a small momentum variation less than 0.02 $Å^{-1}$ which corresponds to 1/80 of the reciprocal lattice vector. This indicates the inherently narrow nature of the QP peak of bulk origin as well as the ultrahigh energy/momentum resolution in the present ARPES measurements. To remove the effect of the Fermi-Dirac distribution function, we symmetrized the ARPES spectra with respect to E_F. The obtained precise momentum dependence of the SC gap [Fig. 2(b)] clearly highlights the $d_{x^2-y^2}$-wave character with a point node at the nodal k_F point in Bi2212.

In order to demonstrate the impurity effect on the low-energy excitations, we show in Figs. 3(a)–3(c) the ARPES intensity at E_F around the node, for (a) pristine, and (b) Zn- and (c) Ni-substituted Bi2212 (Zn- or Ni-Bi2212). The ARPES intensity at E_F was obtained by integrating the spectral intensity within ±1 meV with respect to E_F, and was normalized to the intensity at the energy position of QP peak. As visible in Fig. 3(a), the intensity profile for the pristine sample has an arclike shape, reflecting the position of minimum gap locus which basically tracks the normal-state Fermi surface.[15] The intensity gradually increases with ap-

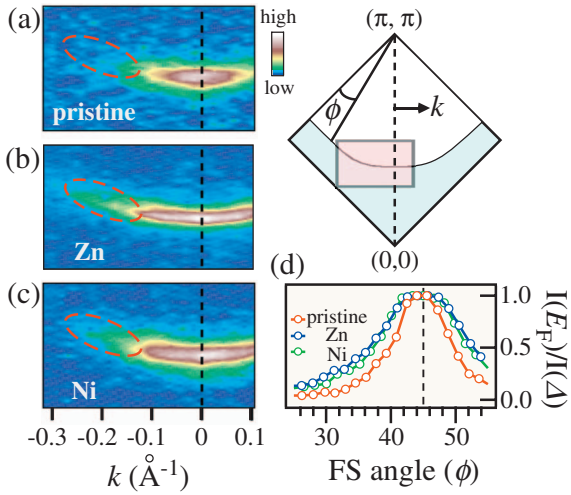

FIG. 3. (Color) ARPES intensity at E_F ($E_F \pm 1$ meV) as a function of 2D wave vector for (a) pristine, (b) Zn-, and (c) Ni-Bi2212, measured at 10 K in the nodal region (area enclosed by a rectangle in the Brillouin zone). The dashed red circles highlight the *k* region where the difference of intensity distribution is most clearly visible. (d) ARPES intensity at E_F with respect to the intensity at the QP-peak position (△), plotted as a function of the Fermi-surface angle (ϕ) of the k_F point, for pristine, Zn-, and Ni-Bi2212.

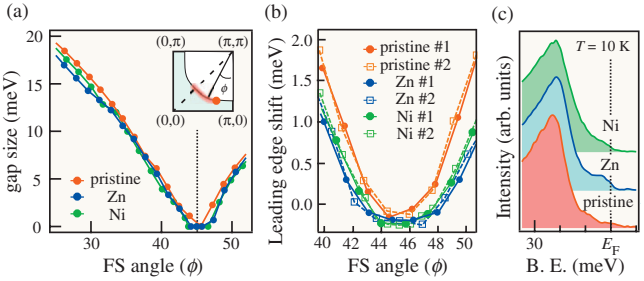

FIG. 4. (Color) (a) Comparison of the k dependence of SC gap ($\triangle$) among pristine, Zn-, and Ni-Bi2212. (b) Leading-edge-midpoint shift around the nodal region. (c) Comparison of 10-K ARPES spectrum in the vicinity of E_F measured at an off-nodal k_F point shown by a red filled circle in the inset of (a).

proaching the node due to the reduction in the SC-gap size (Δ). Upon Zn or Ni substitution [Figs. 3(b) and 3(c)], the intensity-distribution pattern, though it is qualitatively similar to that of the pristine sample, appears to be more widely distributed toward the off-node, as more clearly seen from the comparison of the spectral intensity in the k region enclosed by a dashed red circle in Figs. 3(a)–3(c). This tendency is better illustrated in Fig. 3(d), where the intensity at E_F $[I(E_F)]$ referenced to that at the gap maximum $I(\Delta)$ for various k_F points is plotted as a function of the Fermi-surface angle (ϕ) around the node (ϕ=45°), where ϕ denotes the angle between the k_F-(π,π) and $(\pi,0)-(\pi,\pi)$ lines as shown in the inset. The $I(E_F)/I(\Delta)$ value for Zn- and Ni-Bi2212 is obviously higher than that of the pristine sample, implying the destruction of the SC gap around the node upon impurity doping.

Figure 4(a) shows comparison of the SC-gap size (Δ) as a function of the Fermi-surface angle among pristine, Zn-, and Ni-Bi2212, where Δ is determined by fitting the symmetrized spectra using the phenomenological spectral function including the SC gap size (Δ) and the broadening factor.[16] In addition to the universal $d_{x^2-y^2}$-wave dependence of the SC gap, several small but finite differences among three samples are recognized. First, the gap magnitude in the off-nodal region ($\phi\sim25°$) is slightly (<2 meV) reduced in Zn- and Ni-Bi2212 in comparison with that of the pristine sample. Second, the momentum region where the gap vanishes ($\Delta\sim0$) appears to be a point at ϕ=45° in the pristine sample, while it seems to have a finite width ($44°<\phi<46°$) in both Zn- and Ni-Bi2212. This is also demonstrated in a different way in Fig. 4(b) where the leading-edge-midpoint shift with respect to E_F is plotted as a function of the Fermi-surface angle. We also plot data for different samples of nominally identical composition to demonstrate the reproducibility. The leading-edge rapidly moves away from E_F in the pristine sample when the Fermi-surface angle is increased/decreased from 45°, while it appears to stay at around E_F at ϕ =44–47° in both impurity-doped samples.[17] These results indicate that a point node in pristine Bi2212 evolves into a short gapless Fermi arc upon the impurity doping. In Fig. 4(c), we compare the near-E_F ARPES spectrum measured at 10 K at a k_F point on the off-nodal cut indicated by a red filled circle in the inset of Fig. 4(a). In pristine Bi2212, the spectral intensity is monotonically reduced toward E_F from the QP peak and almost vanishes around E_F. In Zn-Bi2212, on the other hand, a substantial spectral intensity with a clear Fermi-edge cutoff remains at E_F. Interestingly, the Fermi edge is not clearly seen in Ni-Bi2212 in comparison with Zn-Bi2212, demonstrating that Zn and Ni impurities act differently to the low-energy excitations. It is noted here that the evolution of in-gap states in the SC state is observed in both Zn-Bi2212 and Zn-LSCO,[18] suggesting that it is a general feature of hole-doped cuprates. Comparison between these two materials indicates that the in-gap states are less clearly distinguished from the QP peak and the QP peak itself is much weaker in Zn-LSCO than in Zn-Bi2212. These differences are explained by the smaller SC gap size and the higher Zn-impurity concentration in LSCO.[18]

The characteristic change in the gap size upon Zn/Ni substitution as seen in Figs. 4(a) and 4(b) would reflect different aspects of impurity effects between the off-nodal and the nodal region. In the off-nodal region, the reduction in gap size in impurity-substituted samples would be related to the decrease in T_c, while the emergence of a small Fermi arc in the nodal region is caused by the destruction of a small excitation gap due to the strong impurity scattering (pair breaking). The existence of a Fermi arc in impurity-substituted samples obviously violates the ideal $d_{x^2-y^2}$-wave symmetry, demonstrating that the observed gap in Zn- and Ni-Bi2212 cannot be well reproduced by simply assuming a higher-order term of the gap function such as $\cos(6\phi)$ as applied in underdoped Bi2212,[19,20] since the higher-order term never extends the gapless k region around the node. The observed Fermi arc in the SC state is also not reconciled by the two-gap scenario,[21,22] since even in this case the SC gap around the nodal region locally follows the $d_{x^2-y^2}$-wave symmetry with a point node. This suggests that the effect on the SC gap is intrinsically different between impurity and carrier dopings. If the impurity-substitution effect is truly the local phenomenon around the impurity site, it does not modify the overall k dependence of the gap magnitude because such a local effect spreads over the entire k space and has no k dependence. By taking account of the fact that ARPES probes the electronic states averaged over the wide sample-surface area, the impurity-induced reduction in the SC-gap size in the off-nodal region is hardly explained in terms of simple summation of the gap-destroyed states at the impurity site and the impurity-unaffected states far away from the impurity. The experimental result would rather suggest that the electronic states far away from the impurity are also affected by impurities.

While Zn and Ni impurities share a common feature in the effect on the k dependence of the SC gap, they affect the low-energy excitations within the gap in dramatically different manners to each other as shown in Fig. 4(c). The emergence of a Fermi edge in Zn-Bi2212 indicates the existence of in-gap states produced by the QP resonance around Zn impurities.[2] The small Fermi edge in Zn-Bi2212 is observed all over the Brillouin zone with no meaningful momentum variation, indicative of the local character of the in-gap states. On the other hand, the absence of a distinct Fermi edge in Ni-Bi2212 suggests a significantly different scattering potential around the impurity center, which may reflect the energy position of the QP resonance.[2,3] The observed

difference in the distribution of in-gap states between Zn and Ni impurities may be related to the magnetic, transport, and thermodynamic properties. The spectral intensity of in-gap states at E_F is much stronger in Zn-Bi2212 than in Ni-Bi2212, indicating the higher residual DOS at E_F in Zn-Bi2212. This explains well the difference in the electronic specific-heat coefficient γ between Zn- and Ni-substituted $La_{2-x}Sr_xCuO_4$ (Zn/Ni-LSCO),[23] because γ for Zn-LSCO is more rapidly increased than that for Ni-LSCO upon impurity substitution. Nuclear magnetic resonance (NMR) experiments on Zn- and Ni-substituted $YBa_2Cu_3O_{7-\delta}$ suggested that the deduced residual DOS of a Zn-substituted sample is higher than that of a Ni-doped one at the fixed doping level.[24] This NMR observation is consistent with the present ARPES result, showing a clear correlation between the DOS of in-gap states around E_F observed by ARPES and the scattering of QPs inside the SC gap by NMR. Inelastic neutron-scattering (INS) experiments have reported that Zn doping in LSCO produces additional spin excitations of less than 5 meV inside the spin gap at the SC state, while such low-energy spin excitations have not been observed in Ni-LSCO.[25] This remarkable similarity between the INS and the present ARPES results on the characteristic difference between Zn and Ni doping suggests a close correlation between the low-energy spin and the charge excitations within the SC gap.

In conclusion, we have studied the Zn- or Ni-doping effect on the electronic structure near E_F and the superconducting gap in Bi2212 by ARPES. The newly developed Xe plasma light source has enabled the precise bulk-sensitive measurements with high energy and momentum resolutions. We found that the point node near the $(\pi/2,\pi/2)$ in pristine Bi2212 gradually evolves into a small gapless Fermi arc upon the Zn or Ni doping. The observed marked difference in the impurity-induced DOS within the SC gap between Zn and Ni suggests that the low-energy excitation properties are strongly sensitive to the character of impurities.

This work was supported by grants from CREST-JST and MEXT, Japan. K.T. and K.N. thank JSPS for financial support.

[1] M. A. Woolf and F. Reif, Phys. Rev. **137**, A557 (1965).
[2] S. H. Pan, E. W. Hudson, K. M. Lang, H. Eisaki, S. Uchida, and J. C. Davis, Nature (London) **403**, 746 (2000).
[3] E. W. Hudson, K. M. Lang, V. Madhavan, S. H. Pan, H. Eisaki, S. Uchida, and J. C. Davis, Nature (London) **411**, 920 (2001).
[4] A. V. Balatsky, I. Vekhter, and J.-X. Zhu, Rev. Mod. Phys. **78**, 373 (2006).
[5] M. Le Tacon, A. Sacuto, Y. Gallais, D. Colson, and A. Forget, Phys. Rev. B **76**, 144505 (2007).
[6] H. Martinho, A. A. Martin, C. Rettori, and C. T. Lin, Phys. Rev. B **69**, 180501(R) (2004).
[7] N.-C. Yeh, C.-T. Chen, G. Hammerl, J. Mannhart, A. Schmehl, C. W. Schneider, R. R. Schulz, S. Tajima, K. Yoshida, D. Garrigus, and M. Strasik, Phys. Rev. Lett. **87**, 087003 (2001).
[8] M. Limonov, D. Shantsev, S. Tajima, and A. Yamanaka, Phys. Rev. B **65**, 024515 (2001).
[9] S. Souma, T. Sato, T. Takahashi, and P. Baltzer, Rev. Sci. Instrum. **78**, 123104 (2007).
[10] H. Ding, A. F. Bellman, J. C. Campuzano, M. Randeria, M. R. Norman, T. Yokoya, T. Takahashi, H. Katayama-Yoshida, T. Mochiku, K. Kadowaki, G. Jennings, and G. P. Brivio, Phys. Rev. Lett. **76**, 1533 (1996).
[11] D. L. Feng, N. P. Armitage, D. H. Lu, A. Damascelli, J. P. Hu, P. Bogdanov, A. Lanzara, F. Ronning, K. M. Shen, H. Eisaki, C. Kim, J.-i. Shimoyama, K. Kishio, and Z.-X. Shen, Phys. Rev. Lett. **86**, 5550 (2001).
[12] T. Yamasaki, K. Yamazaki, A. Ino, M. Arita, H. Namatame, M. Taniguchi, A. Fujimori, Z.-X. Shen, M. Ishikado, and S. Uchida, Phys. Rev. B **75**, 140513(R) (2007).
[13] A. Damascelli, Z. Hussain, and Z.-X. Shen, Rev. Mod. Phys. **75**, 473 (2003).
[14] J. C. Campuzano, M. R. Norman, and M. Randeria, in *Physics of Conventional and Unconventional Superconductors*, edited by K. H. Bennemann and J. B. Ketterson (Springer-Verlag, Berlin, 2004), Vol. 2, p. 167.
[15] M. R. Norman, H. Ding, M. Randeria, J. C. Campuzano, T. Yokoya, T. Takeuchi, T. Takahashi, T. Mochiku, K. Kadowaki, P. Guptasarma, and D. G. Hinks, Nature (London) **392**, 157 (1998).
[16] M. R. Norman, M. Randeria, H. Ding, and J. C. Campuzano, Phys. Rev. B **57**, R11093 (1998).
[17] When a sharp peak such as a quasiparticle peak is located at/around E_F, the leading-edge midpoint is situated above E_F due to the spectral broadening by the Fermi-Dirac function at finite temperature and the finite energy resolution. This negative leading-edge-midpoint shift has been generally observed in high-resolution ARPES (Ref. 13).
[18] K. Terashima, T. Sato, K. Nakayama, T. Arakane, T. Takahashi, M. Kofu, and K. Hirota, Phys. Rev. B **77**, 092501 (2008).
[19] J. Mesot, M. R. Norman, H. Ding, M. Randeria, J. C. Campuzano, A. Paramekanti, H. M. Fretwell, A. Kaminski, T. Takeuchi, T. Yokoya, T. Sato, T. Takahashi, T. Mochiku, and K. Kadowaki, Phys. Rev. Lett. **83**, 840 (1999).
[20] S. V. Borisenko, A. A. Kordyuk, T. K. Kim, S. Legner, K. A. Nenkov, M. Knupfer, M. S. Golden, J. Fink, H. Berger, and R. Follath, Phys. Rev. B **66**, 140509(R) (2002).
[21] K. Tanaka, W. S. Lee, D. H. Lu, A. Fujimori, T. Fujii, Risdiana, I. Terasaki, D. J. Scalapino, T. P. Devereaux, Z. Hussain, and Z.-X. Shen, Science **314**, 1910 (2006).
[22] W. S. Lee, I. M. Vishik, K. Tanaka, D. H. Lu, T. Sasagawa, N. Nagaosa, T. P. Devereaux, Z. Hussain, and Z.-X. Shen, Nature (London) **450**, 81 (2007).
[23] T. Nakano, N. Momono, T. Nagata, M. Oda, and M. Ido, Phys. Rev. B **58**, 5831 (1998).
[24] Y. Kitaoka, K. Ishida, and K. Asayama, J. Phys. Soc. Jpn. **63**, 2052 (1994).
[25] M. Kofu, H. Kimura, and K. Hirota, Phys. Rev. B **72**, 064502 (2005).